Inactivation of the Nuclear Orphan Receptor COUP-TFII by Small Chemicals.

Rémy Le Guével, Frédérik Oger, Celia P. Martinez-Jimenez, Maud Bizot, Céline Gheeraert, François Firmin, Maheul Ploton, Miroslava Kretova, Gaëlle Palierne, Bart Staels, Peter Barath, Iannis Talianidis, Philippe Lefebvre, Jérôme Eeckhoute, Gilles Salbert

Supporting information

1. Inventory of Supporting Information

- Figure S1: *In silico* analysis of COUP-TFII LBD interaction potential.
- Figure S2: Comparative analysis of COUP-TFII (3cjw), RXRα (1xdk), HNF4α (1m7w), PNR (4log) and TR4 (3p0u) LBD structures.
- Figure S3: Quantification of gel shift experiments.
- Figure S4: Docking of Russig's blue in COUP-TFII surface pocket.
- Supplementary Table I: Nuclear receptor LBD crystallization data.
- Supplementary Experimental Procedures: List of oligonucleotides.
- Supplementary references.
- Supplementary Table II: Focused library of compounds tested in yeast one-hybrid assay.

2. Supplementary Figures and Legends, Tables and Experimental Procedures

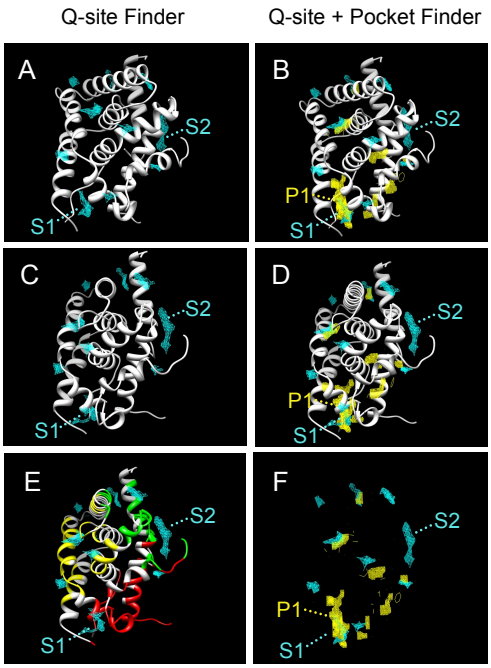

G

Q-site	Vol. Å^3	Pocket	Vol. Å^3
S1	271	P1	208
S2	254	P2	49
S3	153	P3	38
S4	158	P4	31
S5	158	P5	28
S6	134	P6	26
S7	114	P7	25
S8	111	P8	24
S9	113	P9	19
S10	110	P10	19

Figure S1: *In silico* analysis of COUP-TFII LBD interaction potential. Ligand binding sites **(A to F)** and pockets **(B, D and F)** in COUP-TFII LBD (3cjw) were predicted by Q-site Finder and Pocket Finder respectively. Protein-protein interaction surfaces **(E)** were predicted by PPI-Pred. Ligand binding sites are colored in blue, pockets in yellow, and the 3 predicted protein-protein interaction surfaces in yellow, green and red repectively. A and C, as well as B and D, show identical prediction data with a 45° rotation of the protein between two views. The volume of the 10 predicted ligand binding sites and the 10 determined pockets are indicated in **G**.

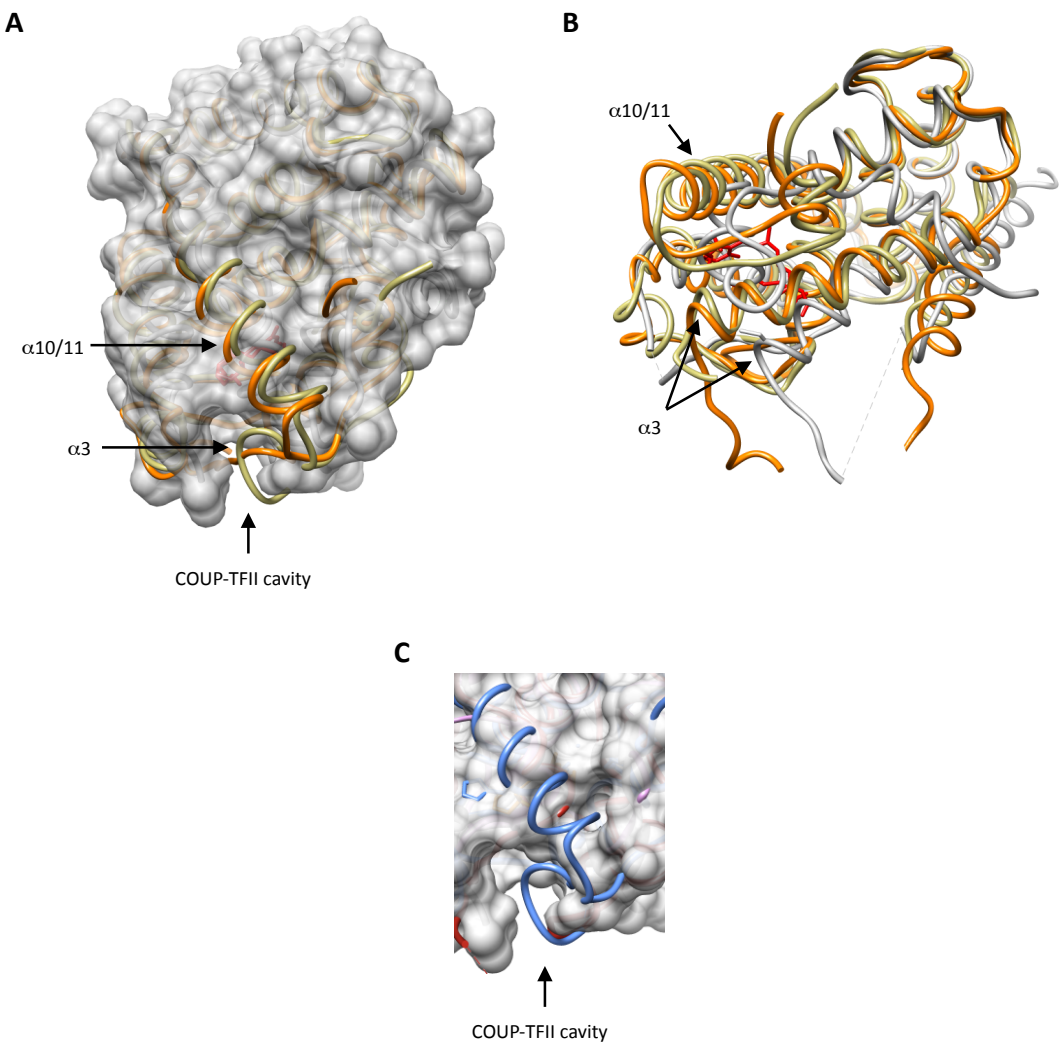

Figure S2: Comparative analysis of COUP-TFII (3cjw), RXRα (1xdk), HNF4α (1m7w), PNR (4log) and TR4 (3p0u) LBD structures. (A) Surface view of COUP-TFII LBD superimposed with ribbon views of RXRα and HNF4α LBDs. Superimposed structures of COUP-TFII LBD is shown in grey, RXRα LBD in kaki and HNF4α LBD in orange. **(B)** Superimposed ribbon views of the 3 NR LBDs. Note that the surface cavity (arrow) found in COUP-TFII LBD structure does not exist in RXRα and HNF4α since this volume is occupied by residues of helix α3 (A and B). Color code is as in **A**. **(C)** Surface view of COUP-TFII LBD (grey), superimposed with ribbon views of RXR (blue), PNR (pink) and TR4 (red) LBDs. Note that only RXR residues fill the space corresponding to the COUP-TFII cavity.

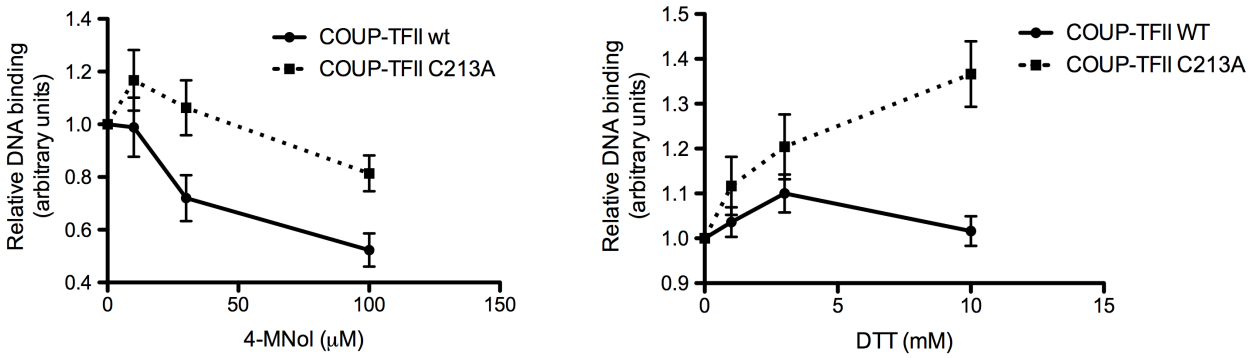

Figure S3: Quantification of gel shift experiments. DNA binding of COUP-TFII wt or C213A was analysed by gel shift assays in the presence of increasing concentrations of 4-MNol (left panel) or DTT (right panel). Images were analysed with the software Image J. Results show the mean +/- SEM of three independent experiments.

A

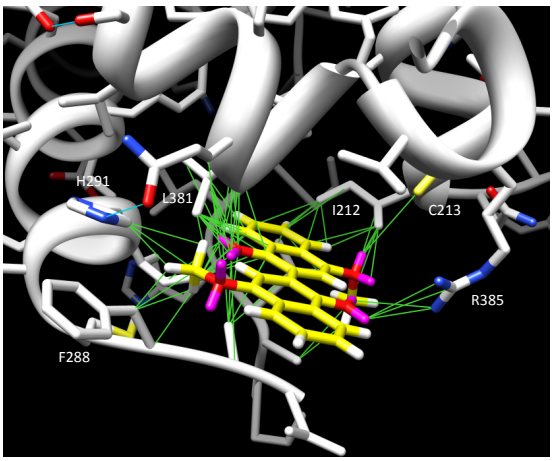

B

	Chemscore	ΔG
4-MNol	16.88	-20.48
Russig's blue	20.39	-25.93

Figure S4: Docking of Russig's blue in COUP-TFII surface pocket. Russig's blue was docked in COUP-TFII LBD cavity with Gold software (Chemscore) and data were visualized with Chimera **(A)**. Residues predicted to establish contact are labeled. Pseudobonds are indicated as green lines. **(B)** Scores and binding energies (kcal/mol) resulting from top solutions from the virtual docking of 4-MNol and Russig's blue into static COUP-TFII LBD (3cjw).

Table I: Nuclear receptor LBD crystallization data								
Protein	nomenclature	resolution Å	ligand	Cavity	Cavity volume Å^3	CoAct/CoRep	PDB	Reference
ERR1	NR3B1	2.5	none	Yes	100	PGC-1	1xb7	Kallen et al. 2004
ERR3	NR3B3	2.7	none	Yes	220	Src-1	1kv6	Greschik et al. 2002
LXR alpha	NR1H3	2.90	T0901317	Yes	700 to 800	NCoA2	1uhl	Svensson et al. 2003
LXRbeta	NR1H2	2.8	epoxycholesterol	Yes	560 to 1090	Src-1	1p8d	Williams et al. 2003
ROR alpha	NR1F1	1.63	cholesterol	Yes	722	none	1n83	Kallen et al. 2002
ROR beta	NR1F2	2.10	ATRA	Yes	766	Src-1	1n4h	Stehlin-Gaon et al. 2003
ROR beta	NR1F2	1.90	stearic acid	Yes	766	Src-1	1k4w	Stehlin et al. 2001
ROR gamma	NR1F3	2.4	hydroxycholesterol	Yes		Src-2	3l0l	Jin et al. 2010
ER alpha	NR3A1	2.4	E2	Yes	490	Tif2	1gwr	Warnmark et al. 2002
ER beta	NR3A2	2.1	E2	Yes	390	NCoA5	2j7x	Pike et al. (PDB only)
FXR	NR1H4	2.5	CDCA	Yes	726	none	1osv	Mi et al., 2003
LRH-1	NR5A2	2.40	none	Yes	820	none	1pk5	Sablin et al. 2003
LRH-1	NR5A2	1.90	Phospholipid	Yes	820	SHP	1yuc	Ortlund et al. 2005
PXR	NR1I2	2.52	none	Yes	1290 to 1540	none	1ilg	Watkins et al. 2001
PXR	NR1I2	2.80	T0901317	Yes	1334	Src-1	2o9i	Xue et al. 2007
PPAR alpha	NR1C1	3.00	GW6471	Yes	1400	SMRT	1kkq	Xu et al. 2002
PPAR gamma	NR1C3	1.99	RO0 p. ag.	Yes	1400	Src-1	2fvj	Burgermeister et al. 2006
PPAR delta	NR1C2	2.50	EPA	Yes	1300	none	1gwx	Xu et al. 1999
SF-1	NR5A1	1.50	Phospholipid	Yes	1600	SHP	1yp0	Li et al. 2005
AR	NR3C4	1.89	R1881 antag.	Yes	450 to 850	Tif2	2ao6	He et al. 2004
RXR alpha	NR2B1	2.7	none	Yes		none	1lbd	Bourguet et al. 1995
RXR alpha	NR2B1	2.25	9-cis RA	Yes	489	none	1fby	Egea et al. 2000
RXR alpha	NR2B1	1.90	BMS 649	Yes	476	NCoA2	1mzn	Egea et al. 2002
RXR alpha	NR2B1	1.90	DHA	Yes	528	NCoA2	1mv9	Egea et al. 2002
RXR beta	NR2B2	2.70	LG100268	Yes	568	none	1h9u	Love et al. 2002
RXR gamma	NR2B3	2.40	none	Yes		none	2gl8	Schuetz et al. (PDB only)
USP*	NR2B4	2.40	phosphatidic acid	Yes	1300	none	1hg4	Clayton et al. 2001
DHR38*	NR4A4	2.40	none	NO	N/A	none	1pdu	Baker et al. 2003
VDR	NR1I1	2.65	calcitriol an.	Yes	870	Src-1	2hbh	Rochel et al. 2007
RAR alpha	NR1B1	2.50	TTNPB	Yes		none	1dkf	Bourguet et al. 2000
RAR beta	NR1B2	2.10	TTNPB	Yes	503	none	1xap	Germain et al. 2004
RAR gamma	NR1B3	1.47	BMS184394	Yes	418	none	1fcx	Klaholz et al. 2000
RAR gamma	NR1B3	2.06	ATRA	Yes	430	none	2lbd	Renaud et al. 1995
MR	NR3C2	1.96	deoxycorticosterone	Yes		none	1y9r	Fagart et al. 2005
PR	NR3C3	1.45	norethindrone	Yes	480	none	1sqn	Madauss et al. 2004
Nurr1	NR4A2	2.20	none	NO	N/A	none	1ovl	Wang et al. 2003
NGF-IB/Nur77	NR4A1	2.40	none	NO	N/A	none	1yje	Flaig et al. 2005
CAR	NR1I3	2.70	pregnanedione	Yes	675	Src-1	1xv9	Xu et al. 2004
TR alpha	NR1A1	2.5	TRb1 agonist	Yes	550	none	1nav	Ye et al. 2003
TR beta1	NR1A2	2.7	TRb1 agonist	Yes	550	none	1nax	Ye et al. 2003
GR	NR3C1	2.50	dexamethasone	Yes	599	Tif2	1m2z	Bledsoe et al. 2002
EcR*	NR1H1	3.07	ponasterone	Yes	766	none	1z5x	Carmichael et al. 2005
HNF4 alpha	NR2A1	2.1	stearic acid	Yes	370	Src-1	1pzl	Duda et al. 2004
HNF4 gamma	NR2A2	2.70	palmitic acid	Yes	626	none	1lv2	Wisely et al. 2002
REV-ERB alpha	NR1D1	2.6	none/heme	NO/yes		NCoR	3n00	Phelan et al. 2010
REV-ERB beta	NR1D2	2.40	none	NO/yes	53 and 26	NCoR	2v7c	Woo et al. 2007
COUP-TFII	NR2F2	1.48	none	NO	N/A	none	3cjw	Kruse et al. 2008
TR4	NR2C2	3.0	none	NO	N/A	none	3p0u	Zhou et al. 2011
PNR	NR2E3	2.8	none	NO	N/A	Src-1	4log	Tan et al. 2013
Uncrystallized mammalian receptors: COUP-TFI, ear 2, GCNF, TR2, TLX, ERR2, MINOR, DAX, SHP								
* indicates drosophila receptors			p. ag.: partial agonist, antag.: antagonist, an.: analogue			N/A: not applicable		

Supplementary Table I: Nuclear receptor LBD crystallization data. * indicates drosophila receptors, p. ag.: partial agonist, antag.: antagonist, an.: analogue, N/A: not applicable. Nuclear receptor LBD with ligand binding pockets under 100 Å^3 or without detectable ligand binding pockets have been highlighted in grey. The CoAct/CoRep column indicates the name of coactivators and corepressors from which peptides have been derived and used for co-crystallization experiments with various LBDs.

Supplementary Experimental Procedures

List of oligonucleotides used for COUP-TFII mutagenesis (Proligo)

I212A up: 5'-CATGGGTATCGAGAACGCTTGCGAACTGGCCGCG-3'

I212A down: 5'-CGCGGCCAGTTCGCAAGCGTTCTCGATACCCATG-3'

W249A up: 5'-CTGCTTCGCCTCACCGCGAGCGAGCTGTTTGTG-3'

W249A down: 5'-CACAAACAGCTCGCTCGCGGTGAGGCGAAGCAG-3'

F253A up: 5'-CACCTGGAGCGAGCTGGCTGTGTTGAATGCGGCG-3'

F253A down: 5'-CGCCGCATTCAACACAGCCAGCTCGCTCCAGGTG-3'

F288A up: 5'-GACCGGGTGGTCGCCGCTATGGACCACATACGG-3'

F288A down: 5'-CCGTATGTGGTCCATAGCGGCGACCACCCGGTC-3'

H291A up: 5'-GTCGCCTTTATGGACGCCATACGGATCTTCCAAGAGC-3'

H291A down: 5'-GCTCTTGGAAGATCCGTATGGCGTCCATAAAGGCGAC-3'

F295A up: 5'-GGACCACATACGGATCGCCCAAGAGCAAGTGGAG-3'

F295A down: 5'-CTCCACTTGCTCTTGGGCGATCCGTATGTGGTCC-3'

C213A up: 5'-GGGTATCGAGAACATAGCTGAACTGGCCGCGAGG-3'

C213A down: 5'-CCTCGCGGCCAGTTCAGCTATGTTCTCGATACCC-3'

List of oligonucleotides used for RT-qPCR (Sigma)

ApoAI up: 5'-TTCTGGCAGCAAGATGAACCC-3'

ApoAI down: 5'-TCAGGCCCTCTGTCTCCTTTT-3'

Cyp7a1 up: 5'-GCAATGAAAGCAGCTACTGAA-3'

Cyp7a1 down: 5'-GTGCATTAACTGTGGGTAAAG-3'

COUP-TFII up: 5'-GCCATAGTCCTGTTCACCT-3'

COUP-TFII down: 5'-GCACACTGAGACTTTTCCTG-3'

RSP28 up: 5'-CGATCCATCATCCGCAATG-3'

RSP28 down: 5'-AGCCAAGCTCAGCGCAAC-3'

List of oligonucleotides used for TaqMan Gene Expression Assays (ThermoFisher Scientific)

Pparg: Mm00440940_m1 probe

Adipoq: Mm00456425_m1 probe

Rn18S: Mm04277571_s1 probe

Supplementary References

Baker, K.D., Shewchuk, L.M., Kozlova, T., Makishima, M., Hassell, A., Wisely, B., Caravella, J.A., Lambert, M.H., Reinking, J.L., Krause, H., Thummel, C.S., Wilson, T.M., and Mangelsdorf, D.J. (2003). The Drosophila orphan nuclear receptor DHR38 mediates an atypical ecdysteroid signaling pathway. *Cell 113*, 731-742.

Bledsoe, R.K., Montana, V.G., Stanley, T.B., Delves, C.J., Apolito, C.J., McKee, D.D., Consler, T.G., Parks, D.J., Stewart, E.L., Willson, T.M., Lambert, M.H., Moore, J.T., Pearce, K.H., and Xu, H.E. (2002). Crystal structure of the glucocorticoid receptor ligand binding domain reveals novel mode of receptor dimerization and coactivator recognition. *Cell 110*, 93-105.

Bourguet, W., Ruff, M., Chambon, P., Gronemeyer, H., and Moras, D. (1995). Crystal structure of the ligand-binding domain of the human nuclear receptor RXR-alpha. *Nature 375*, 377-382.

Bourguet, W., Vivat, V., Wurtz, J.M., Chambon, P., Gronemeyer, H., and Moras D. (2000). Crystal structure of a heterodimeric complex of RAR and RXR ligand-binding domain. *Mol. Cell 5*, 289-298.

Briand, O., Helleboid-Chapman, A., Ploton, M., Hennuyer, N., Carpentier, R., Pattou, F., Vandewalle, B., Moerman, E., Gmyr, V., Kerr-Conte, J., Eeckhoute, J., Staels, B., and Lefebvre, P. **(**2012). The nuclear orphan receptor Nur77 is a lipotoxicity sensor regulating glucose-induced insulin secretion in pancreatic β-cells. *Mol. Endocrinol. 26*, 399-413.

Burgermeister, E., Schnoebelen, A., Flament, A., Benz, J., Stihle, M., Gsell, B., Rufer, A., Ruf, A., Kuhn, B., Märki, H.P., Mizrahi, J., Sebokova, E., Niesor, E, and Meyer, M. (2006). A novel partial agonist of peroxisome proliferator-activated receptor-gamma (PPARgamma) recruits PPARgamma-coactivator-1-alpha, prevents triglyceride accumulation, and potentiates insulin signaling in vitro. *Mol. Endocrinol. 20*, 809-830.

Carmichael, J.A., Lawrence, M.C., Graham, L.D., Pilling, P.A., Epa, V.C., Noyce, L., Lovrecz, G., Winkler, D.A., Pawlak-Skrzecz, A., Eaton, R.E., Hannan, G.N., and Hill, R.J. (2005). The X-ray structure of a hemipteran ecdysone receptor ligand-binding domain: comparison with a lepidopteran

ecdysone receptor ligand-binding domain and implications for insecticide design. *J. Biol. Chem. 280*, 22258-22269.

Clayton, G.M., Peak-Chew, S.Y., Evans, R.M., and Schwabe, J.W. (2001). The structure of the ultraspiracle ligand-binding-domain reveals a nuclear receptor locked in an inactive conformation. *Proc. Natl. Acad. Sci. U.S.A. 98*, 1549-1554.

Duda, K., Chi, Y.I., and Shoelson, S.E. (2004). Structural basis for HNF-4alpha activation by ligand and coactivator binding. *J. Biol. Chem. 279*, 23311-23316.

Egea, P.F., Mitschler, A., Rochel, N., Ruff, M., Chambon, P., and Moras, D. (2000). Crystal structure of the human RXRalpha ligand-binding domain bound to ist natural ligand: 9-cis retinoic acid. *EMBO J. 19*, 2592-2601.

Egea, P.F., Mitschler, A., and Moras, D. (2002). Molecular recognition of agonist ligands by RXRs. *Mol. Endocrinol. 16*, 987-997.

Fagart, J., Huyet, J., Pinon, G.M., Rochel, M., Mayer, C., and Rafestin-Oblin, M.E. (2005). Crystal structure of a mutant mineralocorticoid receptor responsible for hypertension. *Nat. Struct. Mol. Biol. 12*, 554-555.

Flaig, R., Greschik, H., Peluso-Iltis, C., and Moras, D. (2005). Structural basis for the cell-specific activities of the NGFI-B and the Nurr1 ligand-binding domain. *J. Biol. Chem. 280*, 19250-19258.

Germain, P., Kammerer, S., Pérez, E., Peluso-Iltis, C., Tortolani, D., Zusi, F.C., Starrett, J., Lapointe, P., Daris, J.P., Marinier, A., de Lera, A.R., Rochel, N., and Gronemeyer, H. (2004). Rational design of RAR-selective ligands revealed by RARbeta crystal structure. *EMBO Rep. 5*, 877-882.

Greschik, H., Wurtz, J.M., Sanglier, S., Bourguet, W., van Dorsselaer, A., Moras, D., and Renaud, J.P. (2002). Structural and functional evidence for ligand-independent transcriptional activation by the estrogen-related receptor 3. *Mol. Cell 9*, 303-313.

He, B., Gampe, R.T. Jr, Kole, A.J., Hnat, A.T., Stanley, T.B., An, G., Stewart, E.L., Kalman, R.I., Minges, J.T., and Wilson, E.M. (2004). Structural basis for androgen receptor interdomain and coactivator interactions suggests a transition in nuclear receptor activation function dominance. *Mol. Cell 16*, 425-438.

Jin, L., Martynowski, D., Zheng, S., Wada, T., Xie, W., and Li, Y. (2010). Structural basis of hydroxycholesterols as natural ligands of orphan nuclear receptor RORgamma. *Mol. Endocrinol. 24*, 923-929.

Kallen, J.A., Schlaeppi, J.M., Bitsch, F., Geisse, S., Geiser, M., Delhon, I, and Fournier, B. (2002). X-ray structure of the hRORalpha LBD at 1.63 A: structural and functional data that cholesterol or a cholesterol derivative is the natural ligand of RORalpha. *Structure 10*, 1697-1707.

Kallen, J., Schlaeppi, J.M., Bitsch, F., Filipuzzi, I., Schilb, A., Riou, V., Graham, A., Strauss, A., Geiser, M., and Fournier, B. (2004). Evidence for ligand-independent transcriptional activation of the human estrogen-related receptor alpha (ERRalpha): crystal structure of ERRalpha ligand binding domain in complex with peroxisome proliferator-activated receptor coactivator-1 alpha. *J. Biol. Chem. 279*, 49330-49337.

Klaholz, B.P., Mitschler, A., and Moras, D. (2000). Structural basis for isotype selectivity of the human retinoic acid nuclear receptor. *J. Mol. Biol. 302*, 155-170.

Kruse, S.W., Suino-Powell, K., Zhou, X.E., Kretschman, J.E., Reynolds, R., Vonrhein, C., Xu, Y., Wang, L., Tsai, M.J., and Xu, H.E. (2008). Identification of COUP-TFII orphan nuclear receptor as a retinoic acid-activated receptor. *PLoS Biol. 6*, e227.

Li, Y., Choi, M., Cavey, G., Daugherty, J., Suino, K;, Kovach, A., Bingham, N.C., Kliewer, S.A., and Xu, H.E. (2005). Crystallographic identification and functional characterization of phospholipids as ligands for the orphan receptor steroidogenic factor-1. *Mol. Cell 17*, 491-502.

Love, J.D, Gooch, J.T., Benko, S., Li, C., Nagy, L., Chatterjee, V.K., Evans, R.M., and Schwabe, J.W. (2002). The structural basis for the specificity of retinoid-X receptor-selective agonists: new insights into the role of helix H12. *J. Biol. Chem. 277*, 11385-11391.

Madauss, K.P., Deng, S.J., Austin, R.J., Lambert, M.H., McLay, I., Pritchard, J., Short, S.A., Stewart, E.L., Uings, I.J., and Williams, S.P. (2004). Progesterone receptor ligand binding pocket flexibility: crystal structure of the norethindrone and mometasone fuorate complexes. *J. Med. Chem. 47*, 3381-3387.

Mi, L.Z., Devarakonda, S., Harp, J.M., Han, Q., Pelliciari, R., Wilson, T.M., Khorasanizadeh, S., and Rastinejad, F. (2003). Structural basis for bile acid binding and activation of the nuclear receptor FXR. *Mol. Cell 11*, 1093-1100.

Ortlund, E.A., Lee, Y., Solomon, I.H., Hager, J.M., Safi, R., Choi, Y., Guan, Z., Tripathy, A., Raetz, C.R., McDonnell, D.P., Moore, D.D., and Redinbo, M.R. (2005). Modulation of human nuclear receptor LRH-1 activity by phospholipids and SHP. *Nat. Struct. Mol. Biol. 12*, 357-363.

Phelan, C.A., Gampe, R.T. Jr, Lambert, M.H., Parks, D.J., Montana, V., Bynum, J., Broderick, T.M., Hu, X., Williams, S.P., Nolte, R.T., and Lazar, M.A. (2010). Structure of Rev-erbalpha bound to N-CoR reveals a unique mechanism of nuclear receptor-co-receptor interaction. *Nat. Struct. Mol. Biol. 17*, 808-814.

Renaud, J.P., Rochel, N., Ruff, M., Vivat, V., Chambon, P., Gronemeyer, H., and Moras, D. (1995). Crystal structure of the RAR-gamma ligand-binding domain bound to all-trans retinoic acid. *Nature 378*, 681-689.

Rochel, N., Hourai, S., Pérez-Garcia, X., Rumbo, A., Mourino, A., and Moras, D. (2007). Crystal structure of the vitamin D nuclear receptor ligand binding domain in complex with a locked side chain analog of calcitriol. *Arch. Biochem. Biophys. 460*, 172-176.

Sablin, E.P., Krylova, I.N., Fletterick, R.J., and Ingraham, H.A. (2003). Structural basis for ligand-independent activation of the orphan nuclear receptor LRH-1. *Mol. Cell 11*, 1575-1585.

Stehlin, C., Wurtz, J.M., Steinmetz, A., Greiner, E., Schüle, R., Moras, D., and Renaud, J.P. (2001). X-ray structure of the orphan nuclear receptor RORbeta ligand-binding domain in the active conformation. *EMBO J. 20*, 5822-5831.

Stehlin-Gaon, C., Willmann, D., Zeyer, D., Sanglier, S, Van Dorsselaer, A., Renaud, J.P., Moras, D., and Schüle, R. (2003). All-trans retinoic acid is a ligand for the orphan receptor ROR beta. *Nat. Struc. Biol. 10*, 820-825.

Svensson, S., Ostberg, T., Jacobsson, M., Norström, C., Stefansson, K., Hallén, D., Johansson, I.C., Zachrisson, K., Ogg, D., and Jendeberg, L. (2003). Crystal structure of the heterodimeric complex of LXRalpha and RXRbeta ligand-binding domains in a fully agonistic conformation. *EMBO J. 22*, 4625-4633.

Tan, M.H., Zhou, X.E., Soon, F.F., Li, X., Yong, E.L., Melcher, K., and Xu, H.E. (2013). The crystal structure of the orphan nuclear receptor NR3E2/PNR ligand binding domain reveals a dimeric auto-repressed conformation. *PLoS One 8*, e74359.

Wang, Z., Benoit, G., Liu, J., Prasad, S., Aarnisalo, P., Liu, X., Xu, H, Walker, N.P., and Perlmann, T. (2003). Structure and function of Nurr1 identifies a class of ligand-independent nuclear receptors. *Nature 423*, 555-560.

Wärnmark, A., Treuter, E., Gustafsson, J.A., Hubbard, R.E., Brzozowski, A.M., and Pike, A.C. (2002). Interaction of transcriptional intermediary factor 2 nuclear receptor box peptides with the coactivator binding site of estrogen receptor alpha. *J. Biol. Chem. 277*, 21862-21868.

Watkins, R.E., Wisely, G.B., Moore, L.B., Collins, J.L., Lambert, M.H., Williams, S.P., Willson, T.M., Kliewer, S.A., and Redinbo, M.R. (2001). The human nuclear xenobiotic receptor PXR: structural determinants of directed promiscuity. *Science 292*, 2329-2333.

Williams, S., Bledsoe, R.K., Collins, J.L., Boggs, S., Lambert, M.H., Miller, A.B., Moore, J., McKee, DD., Moore, L., Nichols, J., Parks, D., Watson, M., Wisely, B., and Willson, T.M. (2003). X-ray crystal structure of the liver X receptor beta ligand binding domain: regulation by a histidine-tryptophan switch. *J. Biol. Chem. 278*, 27138-27143.

Wisely, G.B., Miller, A.B., Davis, R.G., Thornquest, A.D. Jr, Johnson, R., Spitzer, T., Sefler, A., Shearer, B., Moore, J.T., Miller, A.B., Willson, T.M., and Williams, S.P. (2002). Hepatocyte nuclear factor 4 is a transcription factor that constitutively binds fatty acids. *Structure 10*, 1225-1234.

Woo, E.J., Jeong, D.G., Lim, M.Y., Jun Kim, S., Kim, K.J., Yoon, S.M., Park, B.C., and Ryu, S.E. (2007). Structural insight into the constitutive repression function of the nuclear receptor Rev-erbbeta. *J. Mol. Biol. 373*, 735-744.

Xu, H.E., Lambert, M.H., Montana, V.G., Parks, D.J., Blanchard, S.G., Brown, P.J., Sternbach, D.D., Lehmann, J.M., Wisely, G.B., Willson, T.M., Kliewer, S.A., and Milburn, M.V. (1999). Molecular recognition of fatty acids by peroxisome proliferator-activated receptors. *Mol. Cell 3*, 397-403.

Xu, H.E., Stanley, T.B., Montana, V.G., Lambert, M.H., Shearer, B.G., Cobb, J.E., McKee, D.D., Galardi, C.M., Plunket, K.D., Nolte, R.T., Parks, D.J., Moore, J.T., Kliewer, S.A., Willson, T.M., and Stimmel, J.B. (2002). Structural basis for antagonist-mediated recruitment of nuclear co-repressors by PPARalpha. *Nature 415*, 813-817.

Xu, R.X., Lambert, M.H., Wisely, B.B., Warren, E.N., Weinert, E.E., Waitt, G.M., Williams, J.D., Collins, J.L., Moore, L.B., Willson, T.M., and Moore, J.T. (2004). A structural basis for constitutive activity in the human CAR/RXRalpha heterodimer. *Mol. Cell 16*, 919-928.

Xue, Y., Chao, E., Zuercher, W.J., Willson, T.M., Collins, J.L., and Redinbo, M.R. (2007). Crystal structure of the PXR-T1317 complex provides scaffold to examine the potential for receptor antagonism. *Bioorg. Med. Chem. 15*, 2156-2166.

Ye, L., Li, Y.L., Mellström, K., Mellin, C., Bladh, L.G., Koehler, K., Garg, N., Garcia Collazo, A.M., Litten, C., Husman, B., Persson, K., Ljunggren, J., Grover, G., Sleph, P.G., George, R., and Malm, J. (2003). Thyroid receptor ligands. 1. Agonist ligands selective for the thyroid receptor beta1. *J. Med. Chem. 46*, 1580-1588.

Zhou, X.E., Suino-Powell, K.M., Xu, Y., Chan, C.W., Tanabe, O., Kruse, S.W., Reynolds, R., Engel, J.D., and Xu, H.E. (2011). The orphan nuclear receptor TR4 is a vitamin A-activated nuclear receptor. *J. Biol. Chem. 286*, 2877-2885.

Table II: Focused library of compounds

Compound #	Structure	Name	Characteristics
1	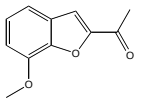	1-(7-methoxybenzofuran-2-yl)ethanone	Chemical Formula: C11H10O3 Exact Mass: 190,06
2	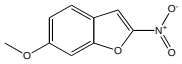	6-methoxy-2-nitrobenzofuran	Chemical Formula: C9H7NO4 Exact Mass: 193,04
3	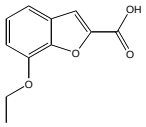	7-ethoxybenzofuran-2-carboxylic acid	Chemical Formula: C11H10O4 Exact Mass: 206,06
4	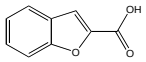	benzofuran-2-carboxylic acid	Chemical Formula: C9H6O3 Exact Mass: 162,03
5	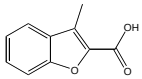	3-methylbenzofuran-2-carboxylic acid	Chemical Formula: C10H8O3 Exact Mass: 176,05
6	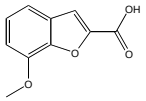	7-methoxybenzofuran-2-carboxylic acid	Chemical Formula: C10H8O4 Exact Mass: 192,04
7	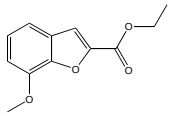	Ethyl 7-methoxybenzofuran-2-carboxylate	Chemical Formula: C12H12O4 Exact Mass: 220,07
8	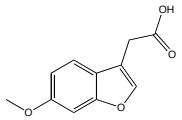	2-(6-methoxy-1-benzofuran-3-yl)acetic acic	Chemical Formula: C11H10O4 Exact Mass: 206,06
9	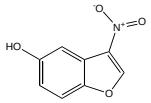	3-nitrobenzofuran-5-ol	Chemical Formula: C8H5NO4 Exact Mass: 179,02
10	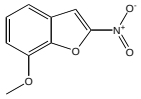	7-methoxy-2-nitrobenzofuran	Chemical Formula: C9H7NO4 Exact Mass: 193,04
11	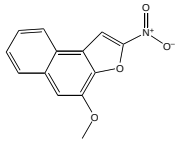	4-methoxy-2-nitronaphtho[2,1-b]furan	Chemical Formula: C13H9NO4 Exact Mass: 243,05
12	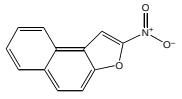	2-nitronaphtho[2,1-b]furan	Chemical Formula: C12H7NO3 Exact Mass: 213,04
13	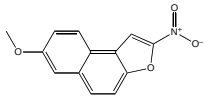	7-methoxy-2-nitronaphtho[2,1-b]furan	Chemical Formula: C13H9NO4 Exact Mass: 243,05
14	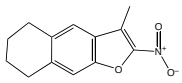	3-methyl-2-nitro-5,6,7,8-tetrahydronaphth [2,3-b]furan	Chemical Formula: C13H13NO3 Exact Mass: 231,09

15	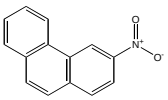	3-nitrophenantrene	Chemical Formula: C14H9NO2 Exact Mass: 223,06
16	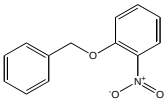	benzyl-2-nitrophenylether	Chemical Formula: C13H11NO3 Exact Mass: 229,07
17	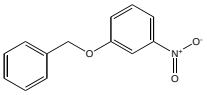	benzyl-3-nitrophenylether	Chemical Formula: C13H11NO3 Exact Mass: 229,07
18	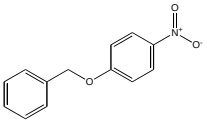	benzyl-4-nitrophenylether	Chemical Formula: C13H11NO3 Exact Mass: 229,07
19	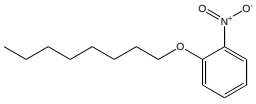	2-nitrophenyl octyl ether	Chemical Formula: C14H21NO3 Exact Mass: 251,15
20	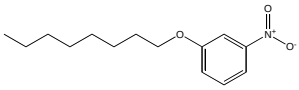	4-nitrophenyl octyl ether	Chemical Formula: C14H21NO3 Exact Mass: 251,15
21	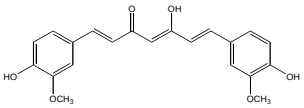	Curcumin	Chemical Formula: C21H20O6 Exact Mass: 368,13
22	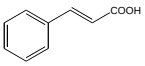	Cinnamic acid	Chemical Formula: C9H8O2 Exact Mass: 148,05
23	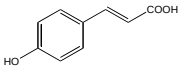	p-Coumaric acid	Chemical Formula: C9H8O3 Exact Mass: 164,05
24	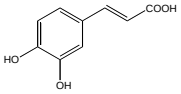	Caffeic acid	Chemical Formula: C9H8O4 Exact Mass: 180,04
25	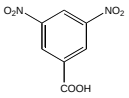	3,5-dinitro-benzoic acid	Chemical Formula: C7H4N2O6 Exact Mass: 212,01
26	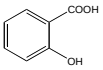	Salicylic acid	Chemical Formula: C7H6O3 Exact Mass: 138,03
27	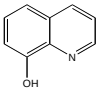	8-hydoxyquinoline	Chemical Formula: C9H7NO Exact Mass: 145,05
28	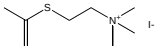	Acetylthiocholine iodide	Chemical Formula: C8H18INS Exact Mass: 287,02
29	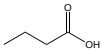	n-Butyric acid	Chemical Formula: C4H8O2 Exact Mass: 88,05
30		DMSO	Chemical Formula: C2H6OS Exact Mass: 78,01

31	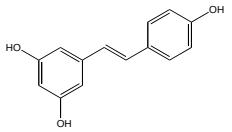	Resveratrol	Chemical Formula: C14H12O3 Exact Mass: 228,08
32	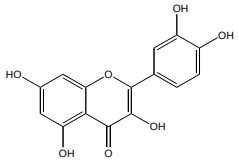	Quercetin	Chemical Formula: C15H10O7 Exact Mass: 302,04
33	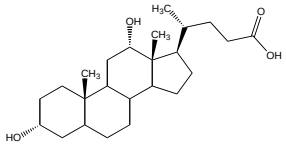	Deoxycholic acid	Chemical Formula: C24H40O4 Exact Mass: 392,29
34	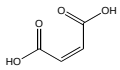	Maleic acid	Chemical Formula: C4H4O4 Exact Mass: 116,01
35		Trichloracetic acid	Chemical Formula: C2HCl3O2 Exact Mass: 161,90
36	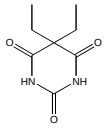	Barbital	Chemical Formula: C8H12N2O3 Exact Mass: 184,08
37	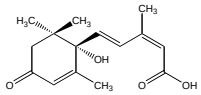	Abscissic acid	Chemical Formula: C15H20O4 Exact Mass: 264,14
38	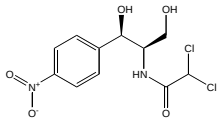	Chloramphenicol	Chemical Formula: C11H12Cl2N2O5 Exact Mass: 322,01
39	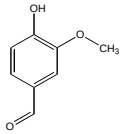	Vanillin	Chemical Formula: C8H8O3 Exact Mass: 152,05
40	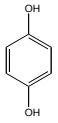	Hydroquinone	Chemical Formula: C6H6O2 Exact Mass: 110,04
41	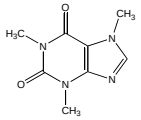	Caffeine	Chemical Formula: C8H10N4O2 Exact Mass: 194,08
42	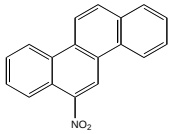	6-Nitrochrysene	Chemical Formula: C18H11NO2 Exact Mass: 273,08

43	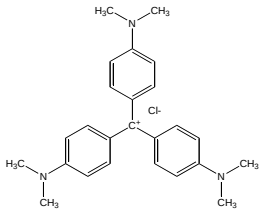	Crystal violet	Chemical Formula: C25H30ClN3 Exact Mass: 407,21
44	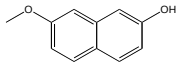	7-methoxynaphthalen-2-ol	Chemical Formula: C11H10O2 Exact Mass: 174,07
45	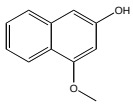	4-methoxynaphthalen-2-ol	Chemical Formula: C11H10O2 Exact Mass: 174,07
46	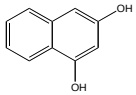	naphthalen-1,3-diol	Chemical Formula: C10H8O2 Exact Mass: 160,05
47	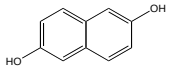	naphthalen-2,6-diol	Chemical Formula: C10H8O2 Exact Mass: 160,05
48	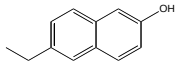	6-ethylnaphthalen-2-ol	Chemical Formula: C12H12O Exact Mass: 172,09
49	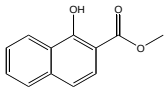	methyl 1-hydroxy-2-naphthoate	Chemical Formula: C12H10O3 Exact Mass: 202,06
50	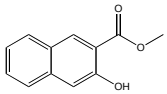	methyl 3-hydroxy-2-naphthoate	Chemical Formula: C12H10O3 Exact Mass: 202,06
51	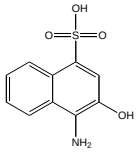	1-amino-2-naphthol-4-sulfonic acid	Chemical Formula: C10H9NO4S Exact Mass: 239,03
52	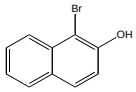	1-bromo-2-naphthol	Chemical Formula: C10H7BrO Exact Mass: 221,97
53	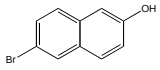	6-bromo-2-naphthol	Chemical Formula: C10H7BrO Exact Mass: 221,97
54	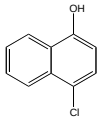	4-chloro-1-naphthol	Chemical Formula: C10H7ClO Exact Mass: 178,02
55	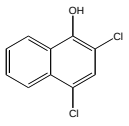	2,4-dichloro-1-naphthol	Chemical Formula: C10H6Cl2O Exact Mass: 211,98

56	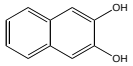	2,3-dihydronaphthalen	Chemical Formula: C10H8O2 Exact Mass: 160,05
57	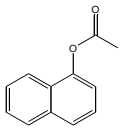	1-naphthyl-acetate	Chemical Formula: C12H10O2 Exact Mass: 186,07
58	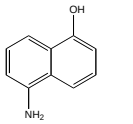	5-amino-1-naphthol	Chemical Formula: C10H9NO Exact Mass: 159,07
59	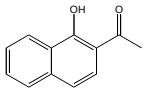	2-acetyl-1-naphthol	Chemical Formula: C12H10O2 Exact Mass: 186,07
60	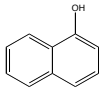	naphthalen-1-ol	Chemical Formula: C10H8O Exact Mass: 144,06
61	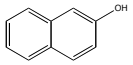	naphthalen-2-ol	Chemical Formula: C10H8O Exact Mass: 144,06
62	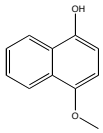	4-methoxynaphthalen-1-ol	Chemical Formula: C11H10O2 Exact Mass: 174,07
63	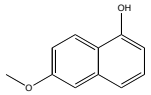	6-methoxynaphthalen-1-ol	Chemical Formula: C11H10O2 Exact Mass: 174,07
64	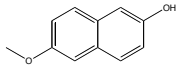	6-methoxynaphthalen-2-ol	Chemical Formula: C11H10O2 Exact Mass: 174,07
65	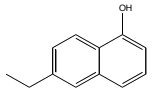	6-ethylnaphthalen-1-ol	Chemical Formula: C12H12O Exact Mass: 172,09
66	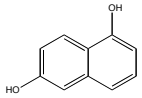	naphthalen-1,6-diol	Chemical Formula: C10H8O2 Exact Mass: 160,05
67	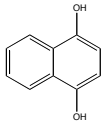	naphthalen-1,4-diol	Chemical Formula: C10H8O2 Exact Mass: 160,05